Groundwater chemistry characterization using multi-criteria approach: The upper Samalà River basin (SW Guatemala)

Groundwater chemistry characterization using multi-criteria approach: the upper Samalá River basin (SW Guatemala)

Arianna Bucci[1], Elisa Franchino[1], Domenico Antonio De Luca[1], Manuela Lasagna[1*], Mery Malandrino[2], Alessandra Bianco Prevot[2], Humberto Osvaldo Hernández Sac[3], Israel Macario Coyoy[4], Edwin Osvaldo Sac Escobar[4], Ardany Hernández[4]

[1] University of Turin, Earth Sciences Department, Via Valperga Caluso 35, 10125 Torino, Italy

[2] University of Turin, Dipartimento di Chimica, Via Pietro Giuria 7, 10125 Torino, Italy

[3] Universidad San Carlos de Guatemala, Centro Universitario de Occidente (CUNOC), Calle Rodolfo Robles 29-99, z.1, Quetzaltenango, Guatemala

[4] Empresa Municipal Aguas de Xelajú (EMAX) 14 Avenida, 6--06 zona 3 Quetzaltenango, Guatemala

* corresponding author (manuela.lasagna@unito.it)

Keywords: groundwater, hydrochemical analyses, chemometrics, principal component analysis, hierarchical clustering analysis, Samalà River

Highlight:

- Groundwater of the upper Samalà River basin (SW Guatemala) have been characterized
- Integrated multi-approach has been used for hydrochemical data interpretation
- Piper, Schoeller and univariate plots were coupled with chemometric tools (PCA, HCA)
- Water quality for drinking purposes did not reveal severe concerns

Abstract

Improving understanding on groundwater chemistry is a key priority for water supply from groundwater resources, especially in developing countries. A hydrochemical study was performed in an area of SW Guatemala (Samalà River basin), where water supply to population is groundwater-based and no systematic studies on its groundwater resources have been performed so far. Traditional hydrochemical analyses on major ions and some trace elements metals coupled with chemometric approach were performed, including principal component analysis and hierarchical clustering analysis. Results evidence that chemical differentiation is linked to the spatial distribution of sampled waters. The most common hydrochemical facies, bicarbonate calcium and magnesium, is linked to infiltration of meteoric waters in recharge areas represented by highlands surrounding Xela caldera, a wide plateau where most of population is concentrated. This trend undergoes chemical evolution in proximity of active volcanic complexes in the southern area, with enrichment in sulphate, chloride and magnesium. Chemical evolution also occurs towards the centre of Xela caldera due to slow circulation in aquifer and consequent sodium enrichment due to ion exchange with the porous medium. Water quality did not reveal severe concerns, even though some sources of contamination could be identified; in particular, agriculture and urban wastewater could be responsible for observed threshold exceedances in nitrate and lead.

This integrated multi-approach to hydrochemical data interpretation yielded to the achievement of important information that poses the basis for future groundwater protection in an area where main water features were almost unknown.

1. Introduction

The assessment of groundwater chemistry in hydrogeological studies allows a better understanding of the influence of geological, climatic features and anthropogenic uses on water composition, allowing to assess the water suitability for drinking, agricultural and industrial purposes. Improving

hydrochemical understanding is thus a key priority for water supply from groundwater resources, especially for those countries characterized by recent urban development and industrial growth as Guatemala. According to CEPAL (2002), water resources volumes in Guatemala is about 201 km^3 of surface water and 34 km^3 of groundwater. In spite of such large availability, current water distribution does not allow the fulfilment of equity, efficiency and environmental sustainability criteria (SEGEPLAN-BID 2006). The upper Samalá River basin, 200 km SW from the capital city, is a wide urban–industrial agglomeration where the risk of groundwater deterioration is high, due to: uncontrolled withdrawal, intense agricultural exploitation, growing industrial activities, untreated waste disposal and uncontrolled discharge of wastewater (CEPAL 2002). Water for human consumption is withdrawn from aquifers because surface waters are used for wastewater discharge, but limited laboratory facilities force most municipalities to detect only basic quality parameters (e.g. pathogenic microorganisms) and only Quetzaltenango city (140k inhabitants) possesses suitable municipal facilities for periodical controls.

Even though groundwater represents the leading resource for human sustainment in Samalà River basin, a chemical characterization at a basin scale for water resources management has not been performed yet. Previous studies give insights about both deep water circulation (Foley et al. 1990, Asturias 2003, Bennati et al. 2011) and groundwater chemistry (Adams et al. 1990, Lima Lobato et al. 2000, Walker et al. 2006). However both studies only aimed at characterizing the fluids of Zunil geothermal reservoir, therefore they are concentrated in a small area 7 km SE from Quetzaltenango. In this scenario, chemical groundwater characterisation would be useful to provide relevant information for groundwater management . In the following, we report the main geological and hydrogeological features of investigation area, which are expected to influence the chemistry of groundwater. Then, the sampling and analytical techniques are described. After that, the main trends of chemical datasets are analysed through classical methods such as classification diagrams (Piper and Schoeller) and bivariate plots. Furthermore an integration with chemometric tools is presented aiming at giving more detailed insights on the hydrochemical features of the investigated

88 area. Indeed, as described by many authors (e.g. Smeti et al. 2009, Kim et al. 2005, 2012,
89 Montcoudiol et al. 2015), large benefits can be obtained in the evaluation of groundwater chemistry
90 and qualitative assessment by joining chemometrics to traditional hydrochemical tools.
91
92 **2. STUDY AREA**
93 **2.1 General setting**
94 Guatemala covers approximately 109,000 km^2 and the estimated population is about 15 million
95 inhabitants, with a growth rate nearly 2% (CIA, 2014), making it the most populous state in Central
96 America. The study area corresponds to the upper Samalá River basin, located 200 km SW from
97 Guatemala City. It represents one of the most populated regions of Guatemala, reaching more than
98 500k inhabitants, a half of whom lives in rural areas in a large number of villages or little
99 communities. The other half lives in towns, the most important ones being Quetzaltenango,
100 Totonicapán and San Juan Ostuncalco (Figure 1). The local economic development is based on
101 husbandry and agriculture and secondarily on craftsmanship, manufacturing and service industries.
102

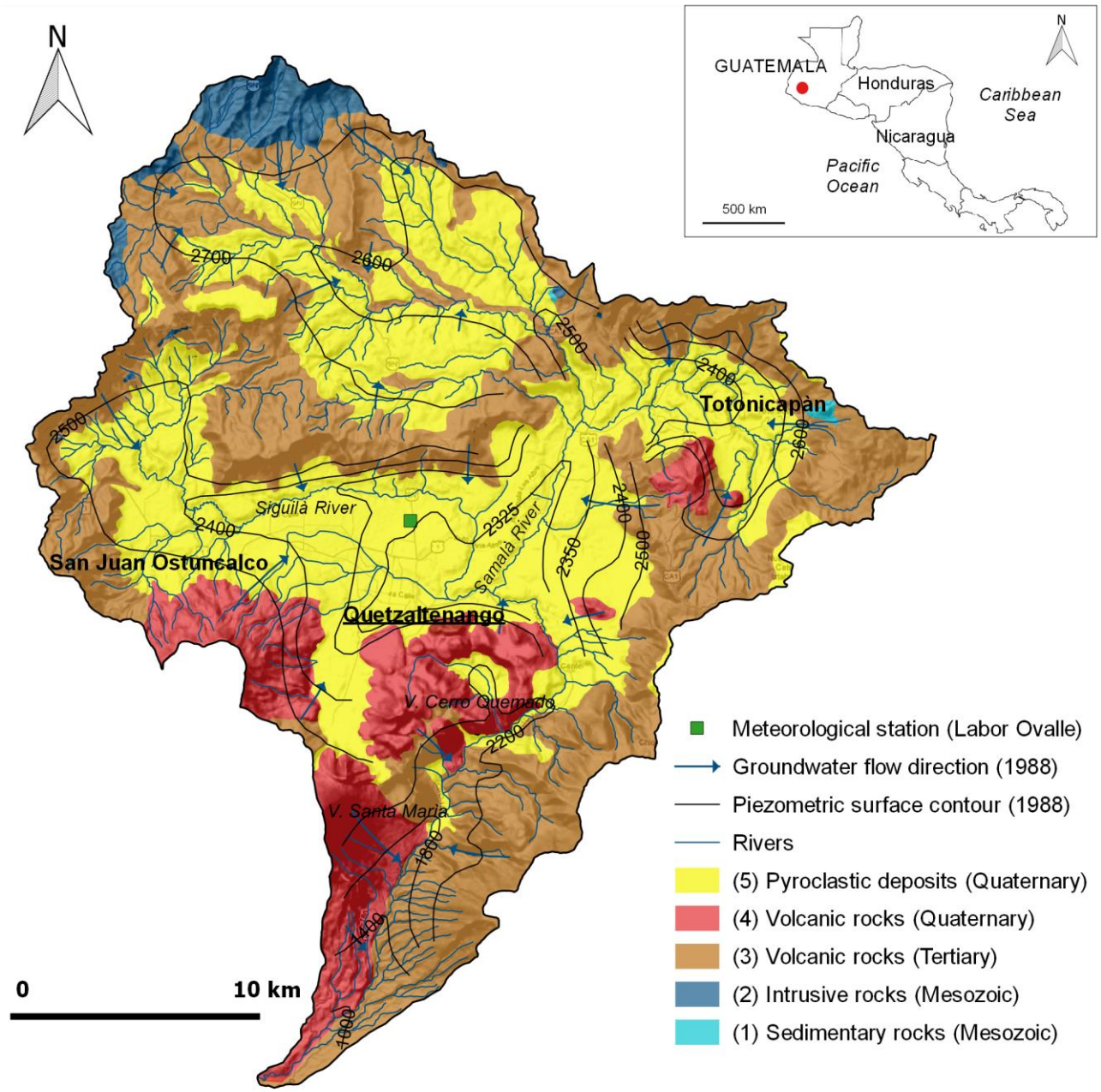

Figure 1. Hydrogeological map showing hydrogeological complexes and potentiometric surface of groundwater represented through iso-piezometric lines and flow direction arrows (adapted from INSIVUMEH 1988)

2.2 Morphology, hydrology and climate

The upper Samalá River basin is located within a volcanic arc called Sierra Madre, where the main volcanoes overtake 3000 meters. The central sector is characterized by a flat or mild morphology, crossed by braided rivers forming fluvial terraces. This region corresponds to an ancient calderic depression (Duffield et al. 1993), named Xela Caldera, remodelled by the rivers action. The hydrographic pattern seems to be essentially controlled by tectonic and volcanic structures, as the Samalá River course displays. It assumes NE-SW direction parallel to Zunil fault zone, then near Quetzaltenango it is deflected by Cerro Quemado volcano and finally it restores NE-SW direction towards south (Figure 1).

The regional climate is typical of tropical highlands, thus with a wet and a dry season and significant variations of temperature and rainfall with respect to the altitude (MARN-URL/IARNA-PNUMA, 2009). Meteorological data from INSIVUMEH Labor Ovalle weather station, located 6 km north of Quetzaltenango at an altitude of 2380 m a.s.l., are summarized in Table 1 and are referred to the temperature and precipitation events data collected in the 1991-2010 period. The average annual rainfall is about 890 mm and the events are mostly concentrated in the rainy season, from May to October, with the highest rainfall in June. Temperature data range between 12.9 °C in January and 15.8 °C in April, with a yearly average of 14.7 °C, and they display small differences among monthly average values. The moisture reaches the maximum at the end of the rainy season in September, with a monthly average of 81.2%.

Table 1. Monthly and annual average air temperature, rainfall and moisture the in upper Samalá River Basin (data from INSIVUMEH weather station Labor Ovalle in the period 1991-2010).

	Jan	Feb	Mar	Apr	May	Jun	Jul	Aug	Sep	Oct	Nov	Dec	Year
Temperature (°C)	12.9	13.7	14.8	15.8	15.8	15.6	15.8	15.8	15.2	15.0	13.4	13.2	14.7
Rainfall (mm)	2.5	2.1	12.9	41.9	142.1	173.3	99.5	115.7	161.6	107.7	21.7	11.2	892.3
Moisture (%)	65.7	63.1	64.5	68.4	74.5	79.4	74.5	76.1	81.2	79.3	72.7	68.6	72.2

2.3 Geological and tectonic setting

The Guatemalan geodynamics consists of a complex interaction between three tectonic plates, North American, Caribbean and Cocos, that originated a NW-SE oriented continental volcanic arc and a wide shear zone with two sub-parallel EW oriented systems of strike-slip faults called Polochic-Motagua (Cáceres et al. 2005, Ortega-Obregón et al. 2008, Phipps Morgan et al. 2008, Bennati et al. 2011). The regional framework is reflected in the study area with the presence of several normal and strike-slip faults, the most significant ones represented by Olintepeque Fault, EW oriented, and the Zunil Fault zone, NE-SW oriented. The southern sector of the area is bordered by various volcanic complexes: Siete Orejas, Santa María-Santiaguito, Cerro Quemado (red sectors in Figure 1). Santa María-Santiaguito and Cerro Quemado complexes showed explosive and effusive activity in historical times (Rose et al. 1987, Conway et al. 1992, Conway et al. 1994, Bennati et al. 2011). The volcanic complexes, together with the aforementioned fault systems, delimit a wide depression identified as Xela Caldera (Duffield et al. 1993). Associated to Zunil fault zone and Xela Caldera eastern margin, a strong hydrothermal activity is found 7 km SE from Quetzaltenango city (Adams et al 1990, Asturias 2003), where several geothermal wells were drilled by the national company for electric supply (INDE).

According to Williams (1960), Rose (1987) and INSIVUMEH (1988), the bedrock is composed by Cretaceous sedimentary and intrusive granitic rocks that rarely outcrop in the northern borders of the investigated area. The most part of the area is constituted by large volumes of effusive

153 intermediate-acid rocks, ignimbrites and pyroclastites that were put in place during the Miocene
154 epoch. The recent and Quaternary volcanic activity was responsible of the formation of high
155 stratovolcanoes and calderic depressions, filled by dacitic and andesitic pyroclastic products derived
156 from explosive eruptions (Williams 1960). The rocky products of both Tertiary and Quaternary
157 eruptions are mainly andesites and basaltic andesites with hornblende and frequently one or two
158 pyroxenes and rarely olivine (Williams 1960, Rose et al. 1977, Rose 1987). The Tertiary
159 volcanoclastic rocks have rhyolitic to rhyo-dacitic composition, while the recent pyroclastic
160 deposits have andesitic to dacitic composition.
161
162 **2.4 Hydrogeological setting**
163 The current limited hydrogeological data availability on the surveyed area makes difficult to
164 reconstruct a deepened hydrogeological conceptual model. However, in this paragraph we will
165 propose a conceptual model according to the existing understanding.
166 According to INSIVUMEH (1988) and Bucci et al. (2015) five hydrogeological complexes can be
167 identified in the upper Samalá River basin (Figure 1): (1) Cretaceous intrusive rocks (Mesozoic
168 granites and granodiorites), (2) Cretaceous sedimentary rocks (terrigenous and calcareous products),
169 (3) Tertiary volcanoclastic and crystalline rocks and (4) Quaternary volcanic rocks, for the most
170 part andesites, and (5) Quaternary pyroclastic deposits.
171 The hydraulic properties of rock masses are not easily definable because of the abundance of factors
172 influencing their hydraulic behaviour as fractured media: the number, the openness and the
173 interconnection of fractures. Igneous rocks are generally characterized by a broad range of
174 hydraulic conductivity values, ranging from 10^{-10} m/s in weathered tuffs to 10^{-4} m/s in fractured
175 basalts (Davis & DeWiest 1966, Spitz & Moreno 1996, Fetter 2001). According to that, Franchino
176 et al. (2013) suggested that the hydraulic conductivity of rocky complexes in the studied area range
177 between low and intermediate, respectively for the older rocky complexes (1), (2) (3) and for

178 Quaternary vulcanites (4), more young and fractured. The presence of hydrothermal circulation in
179 Zunil geothermal fields (Foley 1990, Asturias 2003, Bennati et al. 2011) and of several springs,
180 spread all around the Cerro Quemado Complex (Adams et al. 1990, Lima Lobato et al. 2000,
181 Walker et al. 2006), indicates the presence of groundwater and fluids circulation within the volcanic
182 Cenozoic complexes in fractured and faulted sectors.
183 The Quaternary pyroclastic complex (5) is mainly composed by unconsolidated, coarse-sized
184 pyroclastic products reaching at least 250 meters of depth according to stratigraphic logs of water
185 wells. Rocky and fine-grained ash layers with low permeability are found with unknown lateral
186 extension and thus the aquifer is supposed to be undifferentiated or locally confined. The
187 piezometric surface, showed in Figure 1, is steeper in the foothill sectors, that are supposed to
188 represent the recharge areas. The plain sectors, especially the Xela caldera, where smaller hydraulic
189 gradients occur, represent the discharge areas of groundwater flow; generally, rivers perform as
190 drainage axes. The regional groundwater flow is directed from N to S towards the Pacific Ocean,
191 while locally it turns into NW-SE, SW-NE and E-W directions.
192 The depth to water table in the pyroclastic sediments, inferred from unpublished EMAX (*Empresa*
193 *Municipal de Aguas de Xelajù*) reports, ranges from 3 meters in the eastern suburbs of
194 Quetzaltenango to more than 100 meters in the NW sector of the city. The hydraulic properties of
195 the Quaternary pyroclastic complex have been evaluated from pumping tests carried out by
196 INSIVUMEH, EMAX and IIZ (*Instituto para la Cooperación Internacional de Austria*) in the last
197 30 years all over the upper Samalá River basin. The average hydraulic conductivity is equal to
198 $1.5 \cdot 10^{-5}$ m/s and the average transmissivity is $8.7 \cdot 10^{-3}$ m^2/s, while the storage coefficient ranges
199 between $3 \cdot 10^{-5}$ and $4 \cdot 10^{-5}$.
200 The Quaternary pyroclastic deposits (5) represent the most exploited aquifer due to its favourable
201 hydraulic properties and to its wide distribution. All the water supply of Quetzaltenango
202 municipality is withdrawn from this complex: one quarter (44,500 m^3/day) from Molino Viejo
203 springs -located 7 km NW from Quetzaltenango in Siguilá River Valley- and the remaining from

wells. Molino Viejo springs are tens of water outcrops aligned along the right bank of Siguilá River probably linked with the outcrop of a shallow water table. The exploitation is performed through underground drainage tunnels dug into the pyroclastic sediments and the average discharge is 17 L/s.

3. MATERIALS AND METHODS

3.1 Sampling and chemical analysis

Two sampling surveys were performed in February 2011 and May 2012 within the upper basin of Samalá River. 36 samples were gathered in the first campaign and the remaining 22 during the second one, with 14 common points among the two surveys. The Sampling points consisted of springs and wells owned by municipal authorities and used for drinking purposes. As shown in Table 2, sampled points are mostly wells whose depths range from 70 to 270 meters, while the screens position is mostly unknown. The areal distribution of sampling points (Figure 2) depended on the accessibility of local authorities. Hence, most of the samples were collected in Quetzaltenango city and surroundings. The samples from springs were mostly collected in distal sectors, such as the Molino Viejo group. Each sample point was detailed with a synthetic description and location, acquired through a portable GPS device. Tank and tap sampling points are not included in the presented dataset; when direct sampling was not possible at the water source (well/spring), the water was collected from the inlet pipe upstream the storage tank. The sampled water was collected and stored in 100 mL polyethylene bottles. The main physical-chemical parameters (pH, temperature, electrolytic conductivity, dissolved oxygen) were determined in situ with a HACH portable multi-parameter meter (HQ40d). On the contrary, water analysis were performed in laboratory within few weeks from sample collection. Alkalinity was measured with titration method using 0.1 N HCl. NO_3^-, SO_4^{2-}, Cl^- were determined with a Metrohm ion

chromatography with chemical suppression (Metrosep Dual 4), equipped with a monolithic silica gel column (100x4.6 mm). The eluent (sodium hydrogen carbonate) was provided with a 1 ml/min flux. The instrument was equipped with 863 Compact Autosampler with sampling time equal to 120 s. Before each analysis water was filtered by a 0.45 μm cellulose nitrate membrane filters and after the network was cleaned for 30 s by ethyl alcohol diluted 70% in high-purity water.

The major and minor metal cations (Ca^{2+}, Mg^{2+}, Na^{+}, K^{+}, Mn, Ni and Pb), once the samples were filtered through 0.45 μm cellulose nitrate membrane filters and acidified with HNO_3, were determined by a Perkin Elmer, Optima 7000DV model Inductively Coupled Plasma Atomic Emission Spectrometer (ICP-AES). The instrument is provided with a Echelle monochromator, a cyclonic spray chamber and a teflon Mira Mist nebulizer. The instrumental conditions were: plasma power 1.3 kW; sample aspiration rate 15 rpm; argon nebulizer flow 0.6 L/min; argon auxiliary flow 0.2 L/min and argon plasma flow 15 L/min. All the reagents used were of analytical grade. All metal solutions were prepared from concentrated stock solutions (Sigma Aldrich). High-purity water (HPW) produced with a Millipore Milli-Q Academic system was used throughout.

In order to classify the samples through major ions, data were treated with Piper and Schoeller diagrams and univariate plots. Piper diagram (Piper 1944) is a graphical classification of the chemistry of waters. The cations and anions are plotted in separate ternary plots. The apexes of the cation plot are calcium, magnesium and sodium plus potassium cations. The apexes of the anion plot are sulphate, chloride and carbonate plus hydrogen carbonate anions. The two ternary plots are projected onto a diamond-shape field, that is used to represent the composition of water with respect to both cations and anions. Depending on the position, the hydrochemical facies of the water is defined. The semilogarithmic graph of Schoeller is used to plot the concentrations of anions and cations, in meq/L. The main ionic concentrations are plotted on six equally spaced logarithmic scales, and the points so plotted are joined by straight lines. This diagram gives the absolute concentrations of each ion and allows to make a visual comparison of the compositions of different waters.

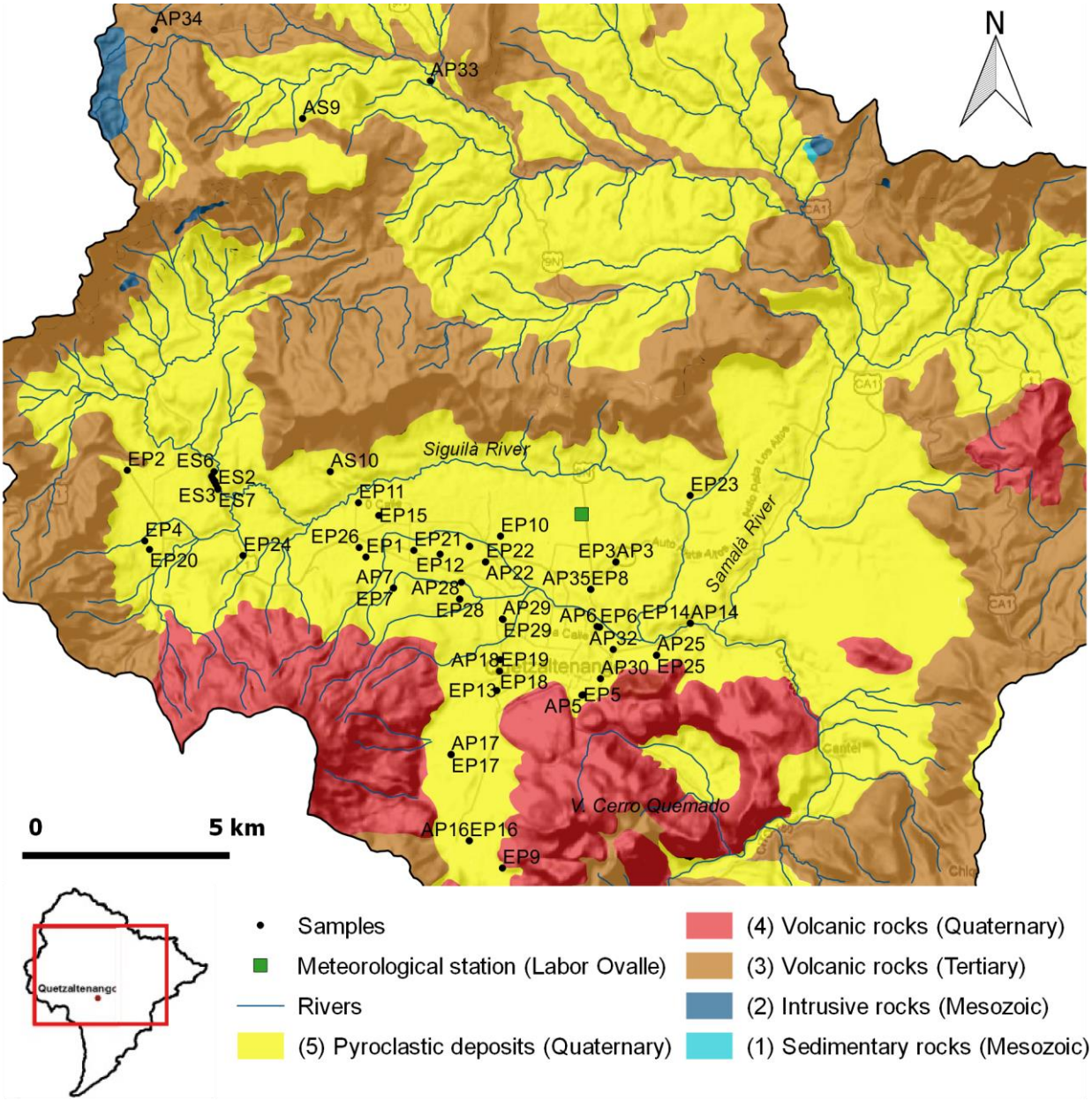

Figure 2. Location of sampling points.

3.2 Chemometric analysis

The chemometric elaboration of the experimental data by principal component analysis (PCA), hierarchical clustering analysis (HCA) and factor analysis (FA) was performed with XlStat 2007.3 software package.

Data set was autoscaled and, when concentrations were below the detection limit, a random value between zero and that limit was inserted in order to be able to thoroughly apply PCA, HCA and FA without losing any data. The variables quantified for less than 70 % of the water samples were not considered further in the chemometric treatment.

PCA is a multivariate chemometric technique used to obtain a synthetic representation of experimental data that brings to light correlations between variables considered and similarities present among samples analysed. This technique makes possible to extract the most information possible contained in a set of multivariate data, summarising it in a few linear combinations of the variables (Einax et al., 2004; Otto M., 2007).

The interpretation of the PCA results can be facilitated through the graphic representation of loading plot and of score plot; in particular, the loading plot allows one to understand the relationships between the variables (in this case the different elements determined in water samples), emphasising their positive and negative correlations and the role of each variable in the different components; the score plot enables the valuation of behaviour of the objects (in this case the samples of analysed water) towards the different components and their similarities or differences.

The aim of HCA is to group data by similarity, taking into account all the information contained in the data set and not only a part of it, as in PCA. Similarity close to 100% indicates high resemblance between the objects, while deviations from a value of 100% indicate differences.

Objects that are most similar are “fused” into a single group or cluster and the calculation of similarity is iteratively repeated. The calculation is interrupted when the minimum similarity (maximum dissimilarity) between the objects has been established. Various graphical means exist to evaluate the aggregation in a cluster, but the most widely used is the dendrogram, which highlights not only the various clusters, but also their distance. The level of aggregation of the units or clusters is visualised in ascending order. HCA is an effective statistical method for qualitative study of the

composition of the waters and can be used to identify the groupings of samples not well detectable only with PCA.

Finally FA is used to explore better the relationship between variables using a Varimax rotation procedure in order to maximise the explained variance.

4. RESULTS AND DISCUSSION

The results of the in situ parameter measurements and chemical analyses are summarised in Table 2. For each sample a list of additional information is given: ID, coordinates, altitude, sampling period, type of sampling point. The sample ID is composed both by letters, that state for the year (E for 2011 and A for 2012) and type of sampling point (S=spring and P=well), and numbers, that identify the sampling location. Water analyses from Adams et al (1990) and Walker et al (2006) are reported in Table 3.

4.1 Physical-chemical parameters

Referring to Table 2, temperature shows a broad variety. Springs have the narrowest range and the lowest values, from 14 to 17.4 °C, while wells temperature varies between 16 and 29°C. Compared to mean annual air temperature of 14.7°C (see Table 1), wells temperatures show higher values. Groundwater temperatures are expected to increase with depth with respect to the external regime, due to the presence of a geothermal heat flux. This seems to be confirmed by the measured values, in most cases ranging 20-21°C. The contribution of geothermal gradient is then more significant than the atmospheric heat input at the depths of the investigated wells between 90 and 280 m (see Table 2). Groundwater temperatures also show some peaks between 23and 29°C concentrated near the active volcanic complexes S. María-Santiaguito and Cerro Quemado. These are likely attributable to anomalous heat fluxes coming from the recent volcanic activity. Nonetheless, correlation between wells depth and temperature is not clear, probably because of water mixing

along the well column due to well screens at various depths. The electrolytic conductivity (EC) assumes values between 52 and 499 μS/cm and an average of 225 μS/cm. The lowest EC values are observed in distal sectors and specifically in springs waters. Conversely, the maxima are concentrated in wells located at the southern sector of the Xela Caldera, near the active volcanic complexes. As for the temperature, a mixing with deep groundwater circuits carrying hot and highly mineralised fluids may be hypothesised. The pH assumes values between 6.98 and 8.10, with a slightly alkaline average of 7.43. Springs generally have slightly acid or neutral pH values, while wells show mostly basic values, with some exceptions from 2012 campaign located close to Cerro Quemado complex.

4.2 Major ions

The analysis of major ions represents a key point in order to understand phenomena and processes involved in defining the groundwater chemical trend. Piper diagram is a powerful tool because it allows to classify groundwater in chemical facies and to compare simultaneously a large number of water samples. Piper diagram (Figure 3) shows that the most part of samples belong to the bicarbonate calcic and magnesiac facies. This is in accordance with typical "young" groundwater composition, that generally starts with alkaline/alkali-earth cations and bicarbonates and gradually evolves towards seawater composition (Appelo & Postma 1996). Thus, the prevalence of HCO_3-Ca-Mg ions can suggest that the most part of groundwater in the investigated area has undergone a short flow path or had limited exchange with the surrounding porous medium and thus its chemistry is mainly governed by infiltration waters (meteoric inputs, streams). The Molino Viejo spring waters are the most representative for this facies since they are grouped at the centre of Ca^{2+}-Mg^{2+}-HCO_3^- water type diamond, suggesting a shallow, rapid groundwater circuit.

Among the waters that display a shift from the general trend, a group of samples -AP5, EP5, AP16, EP16, AP17, AP18- is enriched in Cl^- and SO_4^{2-} and partially in Na^+ and K^+. These samples, contoured with a dashed line in Figure 3, are all located in the area of Cerro Quemado volcanic

complex. This suggests that a possible source of chemical differentiation is related to this active volcano. Here and near Santa María volcano, Walker et al. (2006) observed three main water types: chloride, sulphate, bicarbonate waters. The first ones, according to Adams et al. (1990), were likely originated by various degrees of dilution between shallow, meteoric groundwater and deep hydrothermal Cl^- rich waters that can occur in high-pressure and high-density conditions for condensation of volatile acids and alkali halides (Fournier 1981, Goff & Janik 2000). The sulphate waters in volcanic areas were related to condensation and oxidation of hot and sulphur-rich gases in shallow meteoric waters (White, 1957), while the bicarbonate waters were associated to variable mixing rates between meteoric waters and a high Mg^{2+}-Ca^{2+} volcanic-magmatic component. The Piper diagram also includes samples from Adams et al. (1990) and Walker et al. (2006). The waters come mostly from springs and show a variable chemistry: starting from Ca^{2+}-Mg^{2+}-HCO_3^- facies a progressive enrichments in Cl^- and SO_4^{2-} and in some cases also in Na^+ is observed, up to a composition that approximates the geothermal wells one (yellow pentagons in Figure 3). The enrichment in Cl^-, SO_4^{2-} and partially in Na^+ observed in Piper diagram can be thus originated by mixing between shallow and young groundwater circuits with the volcanic components as end members described by Walker et al. (2006).

The Schoeller diagram in Figure 3 displays all the analysed samples in terms of absolute values of ion concentrations expressed in meq/L. Even though Schoeller diagram is generally represented with few samples, in this case it was chosen to gather all the data in order to evidence common trends and to give an overall idea of absolute ion abundance, lacking in Piper diagram. The main trend, contoured with a dashed line, highlights that the maximum concentrations lie in correspondence of Ca^{2+}, Mg^{2+} and HCO_3^- ions, according to Piper diagram,. The remaining ions generally display lower concentrations, but with more variability. Nitrates, not included in the Piper diagram, show the widest range of concentrations, from 0.001 to approximately 1 meq/L.

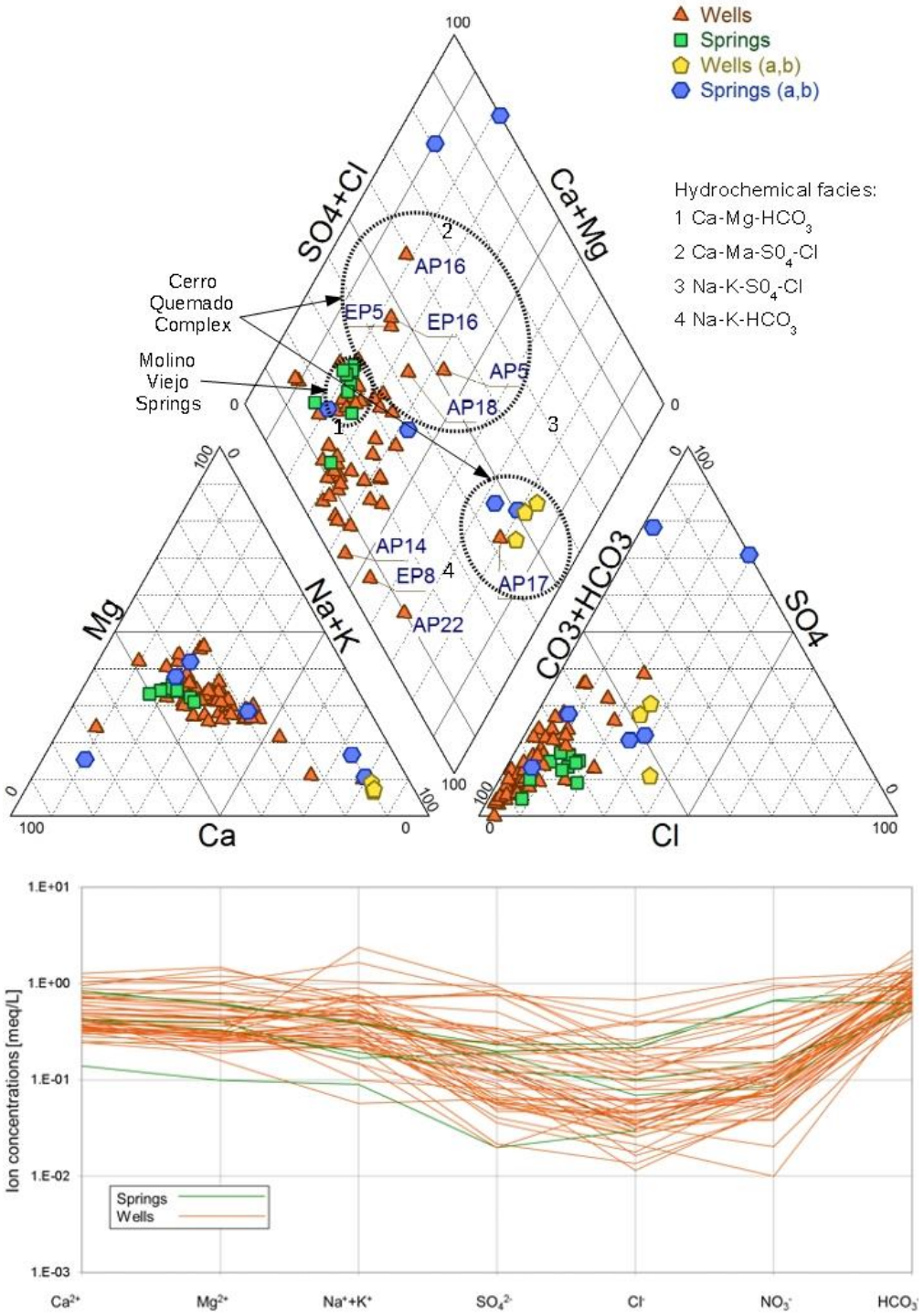

Figure 3. Top: Piper diagram, including the sampled waters and the literature data (a=Walker et al. 2006, b=Adams et al. 1990). Bottom: Schoeller diagram.

In order to better distinguish the factors affecting the chemistry of each water type, major ions were correlated with bivariate diagrams: Na^+-Cl^-, Ca^{2+}-Mg^{2+} and NO_3^--Cl^- (Figure 4). Even in these diagrams we display both ours and Adams et al.'s (1990) and Walker et al.'s (2006) data. The Na^+-Cl^- plot is useful for inferring possible Na inputs, since Na^+ and Cl^- concentrations are generally similar in atmospheric inputs that represent aquifer recharge: according to Möller (1990), continental rainwaters display Na^+ to Cl^- ratios between 1.1 and 1.8. Since our samples are mostly distributed in the uppermost part of the plot, an imbalance towards Na^+ with respect to the chloride occurs due to sodium enrichment from the parental concentrations in rainwater. One possible source of Na^+, already discussed in the previous paragraph, is the mixing with deep hydrothermal circuits for the groundwater around Cerro Quemado complex and indeed these samples are mostly distributed in the uppermost part of Na^+-Cl^- graph. The same samples are also distributed in the uppermost part of the Mg^{2+}-Ca^{2+} plot above the x=y line, indicating that these waters are more enriched in Mg^{2+}. This trend is similar to Walker et al.'s findings, that attributed high Mg^{2+}/Ca^{2+} ratios to an enhanced interaction between meteoric waters in samples collected around the active volcanic complexes.

For the samples far from Cerro Quemado complex, the source of Na^+ ions may be the solid matrix of the main aquifers, formed by andesitic-dacitic pyroclasts and rocks. Strong variations in Na^+-Cl^- ratio from rainwaters to stream waters and groundwater can occur in reason of ion exchange processes with the solid matrix (Neal & Kirchner 2000). As highlighted by Nagaraju et al. (2014), the base ions exchange between groundwater and hosting material during residence or travel can be better understood by studying the chloro-alkaline index. Schoeller (1967) and Schoeller (1977) suggested the chloro-alkaline index CAI_1 in order to understand the direction of such ion exchange processes during the path of groundwater through the aquifer:

$$CAI_1 = [Cl^- - (Na^+ + K^+)]/Cl^-$$

Positive values correspond to depletion of Na^+ and K^+ in the water and an enrichment of Mg^{2+} and Ca^{2+} from the hosting material, whereas negative values occur when the exchange direction is inverse: Mg^{2+} and Ca^{2+} decrease in the water and alkali ions are withdrawn from the porous medium. The CAI_1 index for our samples display values between -0.25 and -18.32 (Table 2), revealing a prevalent Na^+ and K^+ exchange from the rock to the water. The smallest values are displayed by the sampling points within the Xela Caldera. The average values of -6.67 for wells samples and -1.37 for springs samples support the hypothesis that springs are characterized by rapid and short groundwater flow paths, whereas samples from the wells are representative of slower and/or longer paths that facilitate ion exchange processes between water and aquifer matrix. As previously mentioned, the Quaternary pyroclastic sediments filling the Xela caldera contain intercalations of fine volcanic ashes and these fine-size beds likely contain clay minerals that are responsible for ion exchange phenomena in the groundwater.

The different hydrogeology between well and spring waters can be also inferred by the Mg^{2+}-Ca^{2+} plot. Even if the general trend is represented by a prevalence of Ca^{2+} for the samples far from Cerro Quemado complex, some differences can be highlighted among these samples. Spring waters display a more homogeneous pattern: they display lower Mg^{2+} contents compared to the well waters and the Mg^{2+}-Ca^{2+} ratio is rather constant, as showed by their alignment parallel to the $[Mg^{2+}]=[Ca^{2+}]$ line.

As displayed in Table 2, one third of the samples displays nitrates concentrations between 10 and 70 mg/l, significantly above the natural background levels which are typically lower than 1 mg/L of N (corresponding to around 4.4 mg/L of NO_3^-) (Agrawal et al. 1999). This feature, together with the positive correlation between NO^{3-} and Cl^- (Figure 4), are clues of the anthropic origin of both ions, due to synthetic/organic fertilizers and human effluents. As previously mentioned, the study area is characterized by intense agricultural exploitation and lack of sewage network, thus these activities represent diffuse and point sources of both chlorides and nitrates found into the sampled groundwater.

As displayed in Table 2, toxic heavy metals concentrations are mostly around or below 1 ppb. Similar values are typical of non-polluted groundwater and thus significant anthropogenic metal inputs can be excluded in the investigated area. Concerning lead and nickel, the highest concentrations are around 10^{-2} mg/L. In this case an anthropogenic origin is likely, since they were collected within the urbanised area of Quetzaltenango, e.g. for infiltration of urban waste waters enriched in heavy metals. In remote and poorly populated regions some samples (AP33, ES3, ES4, ES7) show higher manganese concentrations around 10^{-2} mg/L compared to the lower quantities of the remaining samples . This higher content of Mn may be due to natural mechanisms of the delicate manganese oxides equilibrium in aquifers, rather than anthropogenic causes.

Table 2 also compares the parameters with Italian and Guatemalan quality standards for drinking purposes. Grey cells highlight exceedances with respect to the assigned thresholds. The two samples exceeding the threshold of lead, already mentioned in the previous paragraph, are linked to urban sources, while the other parameter exceeding the regulatory limits, the nitrates concentration, is often above 50 mg/L. Nitrates are linked to the intense and poorly regulated agricultural/husbandry activities occurring in Quetzaltenango area and to the lack of depuration systems for human wastewaters. A large number of samples shows exceedance for Guatemalan regulation because the nitrates threshold is very strict (10 mg/l), whereas at global level the most frequent limit is 50 mg/L.

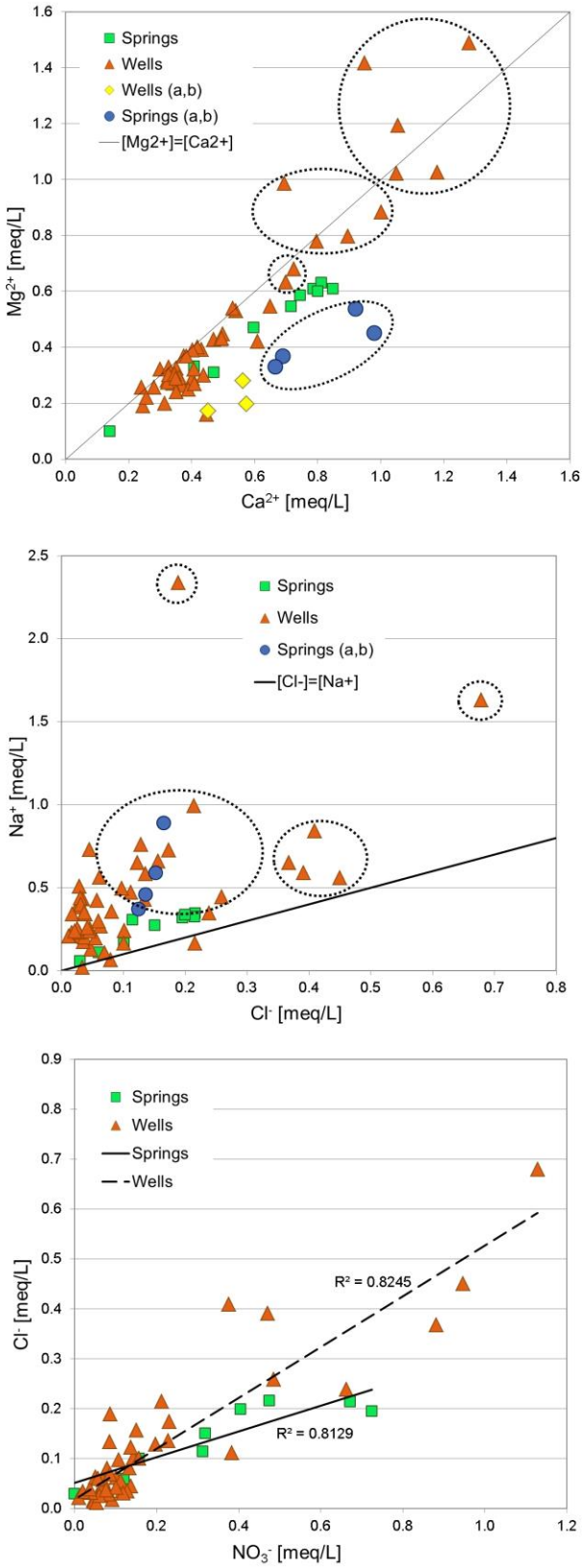

444

445 **Figure 4**. Bivariate plots including sampled waters and literature data. Concentrations are expressed

446 in meq/L. For symbol significance see Fig.3.

447 **Table 2**. Design features of sampling points and main chemical parameters of groundwater samples. Thresholds of drinking water standards are
448 reported in second and third row, for Italy (Legislative Decree 31/2001) and Guatemala (COGUANOR NGO 29.001.98, 1999) respectively.
449

SAMPLE ID	Z (m asl)	TYPE	DEPTH (m bgl)	YEAR	MONTH	T (°C)	EC (µS/cm)	PH	O_2 %	O_2 (mg/L)	Ca^{2+} (mg/L)	Mg^{2+} (mg/L)	Na^{+} (mg/L)	K^{+} (mg/L)	HCO_3^{-} (mg/L)	CO_3^{2-} (mg/L)	SO_4^{2-} (mg/L)	Cl^{-} (mg/L)	NO_3^{-} (mg/L)	TDS (mg/L)	Pb (mg/L)	Ni (mg/L)	Mn (mg/L)	CAI1
IT (D.lgs 31/2001)						34	1500	6.5-8.5			150	100					250	250	50	1000	0.01			
GT (Coguanor, 1999)							2500	6.5-9.5					250				250	250	10		0.01		0.05	
AP14	2327	well	91	2012	May	21.90	158	7.48	58	3.76	5.64	3.13	9.20	1.10	50.32	-	0.00	1.12	2.47	73.04	<0.045E-03	<0.015E-03	2.09E-03	-12.52
AP16	2442	well	213	2012	May	17.40	390	6.97	83	5.84	25.60	18.08	12.87	2.39	56.15	-	41.34	15.97	58.74	214.79	<0.045E-03	<0.015E-03	1.12E-03	-0.38
AP17	2412	well	230	2012	May	20.80	378	7.68	29	1.98	6.54	3.66	9.97	1.75	91.89	-	45.44	6.70	5.39	171.74	<0.045E-03	<0.015E-03	1.67E-03	-11.59
AP18	2391	well	183	2012	May	23.80	322	7.31	69	4.33	14.01	7.70	15.16	1.97	72.20	-	36.17	5.55	9.39	162.23	<0.045E-03	<0.015E-03	1.10E-03	-3.53
AP22	2402	well	185	2012	May	24.20	175	7.45	83	5.23	4.73	1.39	14.58	2.12	54.69	-	2.76	1.39	2.34	84.06	<0.045E-03	<0.015E-03	1.09E-03	-8.83
AP25	2393	well	171	2012	May	26.10	230	7.59	76	4.58	10.60	6.48	9.89	3.39	56.15	-	14.17	4.75	5.28	100.27	<0.045E-03	<0.015E-03	1.23E-03	-2.85
AP27	2419	well	247	2012	May	23.20	174	7.32	80	4.94	7.80	3.04	6.90	1.43	49.59	-	4.77	2.12	3.54	79.24	3.29E-03	<0.015E-03	1.54E-03	-4.64
AP28	2462	well		2012	May	22.10	172	7.47	89	5.65	6.13	4.11	9.82	2.24	47.40	-	5.54	1.49	6.27	83.08	<0.045E-03	<0.015E-03	1.82E-03	-6.34
AP29	2405	well	183	2012	May	23.00	178	7.39	87	5.56	6.90	3.45	8.05	1.90	50.32	-	6.98	1.31	4.81	92.01	<0.045E-03	<0.015E-03	1.15E-03	-9.54
AP3	2349	well	213	2012	May	20.50	174	7.48	78	5.20	9.92	5.25	1.50	1.35	51.63	-	3.88	2.83	4.92	81.44	<0.045E-03	<0.015E-03	1.11E-03	-0.25
AP30	2361	well	137	2012	May	22.50	266	7.41	-	-	10.83	6.45	16.73	1.57	64.17	-	13.80	6.16	14.30	134.08	6.33E-03	6.33E-06	1.56E-03	-3.42
AP31	2432	well	160	2012	May	21.30	193	7.35	77	6.95	7.52	4.47	11.41	1.71	53.24	-	7.44	3.45	6.72	96.07	<0.045E-03	<0.015E-03	9.84E-04	-4.55
AP32	2329	well	140	2012	May	23.30	219	7.47	84	5.35	8.07	4.74	14.94	1.28	61.99	-	5.69	4.35	8.49	109.62	1.35E-02	1.35E-05	2.69E-03	-4.56
AP33	2612	well		2012	May	24.70	141	7.49	26	1.57	7.04	2.92	5.49	1.92	44.48	-	1.94	0.76	0.62	61.31	5.07E-04	5.07E-07	1.86E-02	-12.46
AP34	2788	well		2012	May	15.90	97	7.24	105	7.54	8.96	1.94	0.46	1.44	32.09	-	3.07	1.20	1.26	50.44	<0.045E-03	<0.015E-03	1.23E-03	-0.68
AP35	2309	well	183	2012	May	26.70	178	7.70	69	4.09	7.68	4.47	6.21	2.26	55.42	-	3.00	2.24	3.16	84.52	1.28E-03	<0.015E-03	1.74E-03	-4.18
AP5	2314	well	122	2012	May	21.10	398	7.02	74	4.76	23.62	12.47	37.51	1.24	80.95	-	36.43	24.07	69.97	286.51	<0.045E-03	<0.015E-03	1.14E-03	-1.45
AP6	2349	well	76	2012	May	21.80	349	7.28	76	5.07	15.97	9.46	19.36	2.22	78.61	-	12.17	14.52	23.28	175.73	<0.045E-03	<0.015E-03	2.38E-03	-1.19
AP7	2514	well	201	2012	May	20.20	150	7.52	100	6.95	8.40	4.86	2.46	2.40	40.84	-	9.25	2.47	5.36	76.14	<0.045E-03	<0.015E-03	1.09E-03	-1.42
AS10	2427	spring		2012	May	16.90	147	7.10	85	5.95	9.43	3.75	10.35	1.75	40.11	-	3.81	2.01	7.16	78.40	<0.045E-03	<0.015E-03	1.29E-03	-1.50
AS4	2436	spring		2012	May	16.30	238	6.73	91	6.47	18.56	8.16	6.67	3.24	55.42	-	5.53	8.46	41.07	132.74	<0.045E-03	<0.015E-03	9.56E-04	-0.63
AS9	2766	spring		2012	May	13.80	52	7.29	97	7.27	2.71	1.25	1.41	1.28	18.23	-	0.77	0.96	0.06	26.71	<0.045E-03	2.64E-03	1.50E-03	-2.00
EP1	2486	well		2011	February	22.70	202	7.91	104	6.83	4.92	2.31	5.27	0.58	27.58	-	6.94	0.58	2.84	51.02	3.80E-03	<0.015E-03	8.83E-03	-13.86

EP10	2402	well	183	2011	February	24.80	160	7.70	91	5.62	5.13	2.68	4.76	0.57	36.73	-	1.04	0.48	2.95	54.35	7.55E-03	<0.015E-03	<2.0E-06	-15.34
EP11	2480	well	168	2011	February	21.50	198	7.30	64	4.36	8.07	3.52	8.81	1.28	47.11	-	10.37	0.93	4.04	84.12	6.39E-03	<0.015E-03	<2.0E-06	-14.92
EP12	2443	well	138	2011	February	23.50	204	7.54	80	5.12	7.38	3.21	4.66	0.62	39.84	-	3.47	1.32	4.17	64.68	1.84E-03	<0.015E-03	<2.0E-06	-4.88
EP13	2370	well	213	2011	February	29.30	282	7.51	88	5.02	17.95	9.68	13.42	2.23	100.19	-	24.46	4.82	14.13	186.89	6.84E-03	1.61E-03	1.10E-03	-3.71
EP14	2318	well	91	2011	February	20.60	160	7.72	65	4.43	6.47	3.42	7.86	0.42	48.14	-	1.72	0.63	5.69	74.35	1.38E-03	<0.015E-03	8.66E-03	-18.75
EP15	2479	well	156	2011	February	22.50	191	7.67	76	4.92	6.31	2.43	4.81	0.53	39.03	-	4.50	0.41	3.33	61.35	3.01E-03	<0.015E-03	<2.0E-06	-18.32
EP16	2457	well	213	2011	February	16.80	387	7.19	80	5.64	19.02	17.22	15.00	2.70	80.18	-	37.56	13.03	54.65	239.36	7.11E-03	1.71E-03	1.45E-03	-0.96
EP17	2406	well	230	2011	February	20.20	453	8.10	78	5.16	21.12	14.51	22.86	1.84	122.83	5.70	44.82	7.60	13.14	254.42	6.84E-03	1.74E-03	5.70E-03	-3.86
EP18	2362	well	183	2011	February	24.30	334	7.65	73	4.58	20.07	10.75	17.45	2.09	111.30	-	34.32	4.56	12.28	212.81	2.75E-03	1.16E-03	2.93E-04	-5.32
EP19	2375	well	67	2011	February	21.70	284	7.62	85	5.61	12.99	6.64	8.22	1.25	59.74	-	15.71	2.88	8.27	115.69	3.67E-03	<0.015E-03	5.49E-04	-3.80
EP2	2520	well	213	2011	February	17.50	199	7.00	89	6.29	6.01	3.92	2.98	0.70	33.19	-	2.79	1.70	4.39	55.68	6.94E-03	<0.015E-03	<2.0E-06	-2.08
EP20	2506	well	187	2011	February	20.60	175	7.36	99	6.61	7.05	3.95	4.48	1.11	35.15	-	6.02	1.95	6.99	66.70	5.61E-03	<0.015E-03	<2.0E-06	-3.06
EP21	2455	well	183	2011	February	23.90	183	7.58	87	5.47	6.81	3.30	5.33	0.87	39.91	-	4.17	1.03	4.93	66.35	3.94E-03	<0.015E-03	4.99E-03	-7.75
EP22	2411	well	185	2011	February	26.00	171	7.72	83	5.13	9.40	5.20	11.66	1.41	82.43	-	2.93	1.03	5.15	119.21	9.01E-03	1.35E-03	8.69E-03	-17.78
EP23	2336	well	78	2011	February	17.50	168	7.85	85	6.08	8.17	3.91	5.80	0.37	47.96	-	2.43	1.65	4.29	74.58	5.04E-03	<0.015E-03	5.66E-03	-4.64
EP24	2502	well	198	2011	February	18.80	225	6.72	97	6.72	12.21	5.12	5.57	1.37	43.44	-	12.03	3.61	8.86	92.22	3.89E-03	<0.015E-03	<2.0E-06	-1.72
EP25	2401	well	171	2011	February	21.00	238	7.74	68	4.63	6.49	3.34	9.75	0.78	45.03	-	7.42	2.03	4.36	79.20	9.31E-04	<0.015E-03	1.12E-03	-6.76
EP26	2468	well	156	2011	February	18.70	218	7.94	103	7.10	8.76	3.65	5.52	0.95	37.53	-	8.49	1.60	8.48	74.98	8.18E-03	<0.015E-03	<2.0E-06	-4.84
EP27	2423	well	247	2011	February	26.90	164	7.54	83	5.03	7.22	3.55	5.86	0.86	46.25	-	2.66	0.91	3.80	71.11	8.72E-04	<0.015E-03	<2.0E-06	-9.80
EP28	2446	well		2011	February	21.90	173	7.79	88	5.74	9.85	5.23	9.92	1.58	74.07	-	5.33	1.23	7.95	115.17	5.50E-03	1.68E-03	5.96E-03	-12.65
EP29	2411	well	183	2011	February	22.80	177	7.80	96	6.19	10.00	5.45	10.12	1.68	76.03	-	6.77	1.09	7.36	118.51	9.06E-03	1.52E-03	1.09E-03	-14.65
EP3	2382	well	213	2011	February	17.10	166	7.74	71	5.20	8.65	4.76	12.96	1.20	81.03	-	3.16	2.19	6.27	120.21	2.17E-03	1.19E-03	7.98E-04	-8.63
EP4	2533	well	183	2011	February	24.80	174	7.51	93	5.66	4.84	3.12	4.80	1.19	34.66	-	2.74	0.93	3.44	55.72	5.27E-03	<0.015E-03	<2.0E-06	-8.09
EP5	2341	well	122	2011	February	20.90	499	7.38	65	4.44	14.52	8.26	10.23	0.26	43.87	-	16.32	9.17	30.11	132.74	9.42E-04	<0.015E-03	1.14E-03	-0.75
EP6	2327	well	76	2011	February	21.80	340	7.55	80	5.30	21.02	12.43	13.57	2.03	111.84	-	11.46	13.88	29.21	215.44	6.09E-03	2.24E-03	3.39E-03	-0.64
EP7	2506	well	201	2011	February	20.00	151	7.76	98	6.48	6.57	3.99	3.99	0.83	34.96	-	5.66	1.25	7.19	64.44	6.18E-03	<0.015E-03	1.59E-04	-4.53
EP8	2381	well	183	2011	February	26.20	175	7.91	99	6.40	7.15	3.66	16.79	1.12	81.88	-	2.26	1.60	4.73	119.20	2.77E-03	4.08E-04	1.49E-03	-15.85
EP9	2466	well	244	2011	February	20.50	271	7.03	84	5.74	13.92	11.98	10.88	0.78	89.45	-	16.62	3.97	23.75	171.35	2.07E-02	1.30E-02	3.25E-04	-3.41
ES1	2443	spring		2011	February	16.50	210	6.98	94	6.89	8.17	4.04	3.82	1.12	32.09	-	5.97	3.57	9.70	68.49	4.40E-03	<0.015E-03	<2.0E-06	-0.94
ES2	2440	spring		2011	February	16.80	230	7.04	93	6.81	15.73	7.42	8.02	2.31	65.35	-	9.58	7.67	29.42	145.50	3.54E-03	1.43E-03	2.05E-03	-0.89
ES3	2445	spring		2011	February	15.90	238	7.18	92	6.75	16.25	7.67	7.50	2.22	54.67	-	9.45	7.62	41.63	147.01	6.35E-03	1.70E-03	2.60E-02	-0.78
ES4	2448	spring		2011	February	16.10	230	7.02	92	6.70	16.03	7.31	7.40	2.07	52.23	-	8.49	6.94	44.94	145.41	4.08E-03	1.27E-03	1.02E-02	-0.92
ES5	2442	spring		2011	February	16.30	178	7.11	92	6.72	11.95	5.72	7.06	3.27	55.59	-	8.59	4.06	19.33	115.57	6.94E-03	1.21E-03	6.15E-05	-2.41
ES6	2437	spring		2011	February	16.40	230	7.03	91	6.71	14.32	6.64	6.29	1.75	59.92	-	11.32	5.35	19.76	125.34	5.18E-03	2.21E-03	6.60E-03	-1.11
ES7	2435	spring		2011	February	16.70	206	7.26	95	6.80	14.90	7.13	7.76	2.27	66.14	-	8.87	7.07	25.07	139.21	6.45E-03	2.39E-03	4.83E-02	-0.98

450 **Table 3.** Chemical parameters of groundwater investigated by Adams (1990) and Walker (2006).
451 Analyses are not balanced.
452

SAMPLE ID	TYPE	LOCATION NAME	Ca2+ (mg/L)	Mg2+ (mg/L)	Na+ (mg/L)	K+ (mg/L)	HCO3- (mg/L)	SO42- (mg/L)	Cl- (mg/L)	TDS	T (°C)	pH
ZTG-38	spring	Llano del Pinal	92.9	11.6	13.5	2.0	72.0	230.0	5.3	427.3	14.9	6.0
ZTG-15	spring	Chicua	19.6	10.8	8.5	4.5	98.8	12.7	4.4	159.3	14.4	6.5
ZTG-19	spring	Zunil	40.2	40.0	313.0	32.0	665.0	202.0	186.0	1478.2	74.4	7.8
ZTG-28	spring	Zunil	13.8	8.8	116.0	14.4	210.0	73.2	70.8	507.0	61.4	7.0
95-B4	spring	Zunil	18.4	12.9	10.5	3.9	0.0	15.8	4.8	68.0	25.5	6.3
95-B2	well	Almolonga	11.3	6.7	110.1	6.2	182.9	82.5	55.1	455.8	38.9	6.2
95-B9	well	Baños Cirilo Flores	11.5	4.7	105.8	7.5	140.5	77.1	48.4	395.9	48.5	6.9
95-B10	well	Baños Chocovi	9.0	4.1	82.6	12.3	141.7	22.6	54.6	327.0	47.1	7.5
95-B28	spring	Inde Dam	13.3	7.9	20.4	3.5	83.64	28.4	5.8	172.2	18.7	10.0

453
454
455 **4.3 Results of chemometric analysis**
456 The univariate analysis of the chemical dataset presented in the previous paragraph was not
457 sufficient to fully describe the groundwater features. A clear identification of the factors influencing
458 the hydrogeochemistry of the studied area, as well as the relationship between chemical behaviour
459 and spatial distribution of samples, were still missing. Thus, a new approach to the dataset through
460 multivariate techniques was adopted.
461 In order to distinguish similar chemical behaviours among the sampled waters, not detected through
462 univariate analysis described in the previous paragraph, a HCA was performed. The similarity
463 between objects was measured by squared Euclidean distances, and the Ward's method of
464 agglomerative HCA was used. Figure 5 displays the results of the HCA analysis on the whole
465 sample set. Three clusters, named C1, C2 and C3 from the bottom to the top of the dendrogram, can
466 be distinguished. The majority of samples (43) are grouped in cluster C1. These samples come from
467 31 different wells, almost entirely located in the central sector of Xela Caldera, among which 8
468 were sampled in both the two campaigns and three springs (ES1, AS9, AS10). At bottom of this
469 cluster it is possible to distinguish a smaller grouping characterized by higher dissimilarity and

composed by three samples: EP17, AP5 whose location is nearby the active volcanic complexes, and AP33, collected in the northern part of the study area, 15 km from the others.

The cluster C2 is entirely composed by springs water in Molino Viejo area.

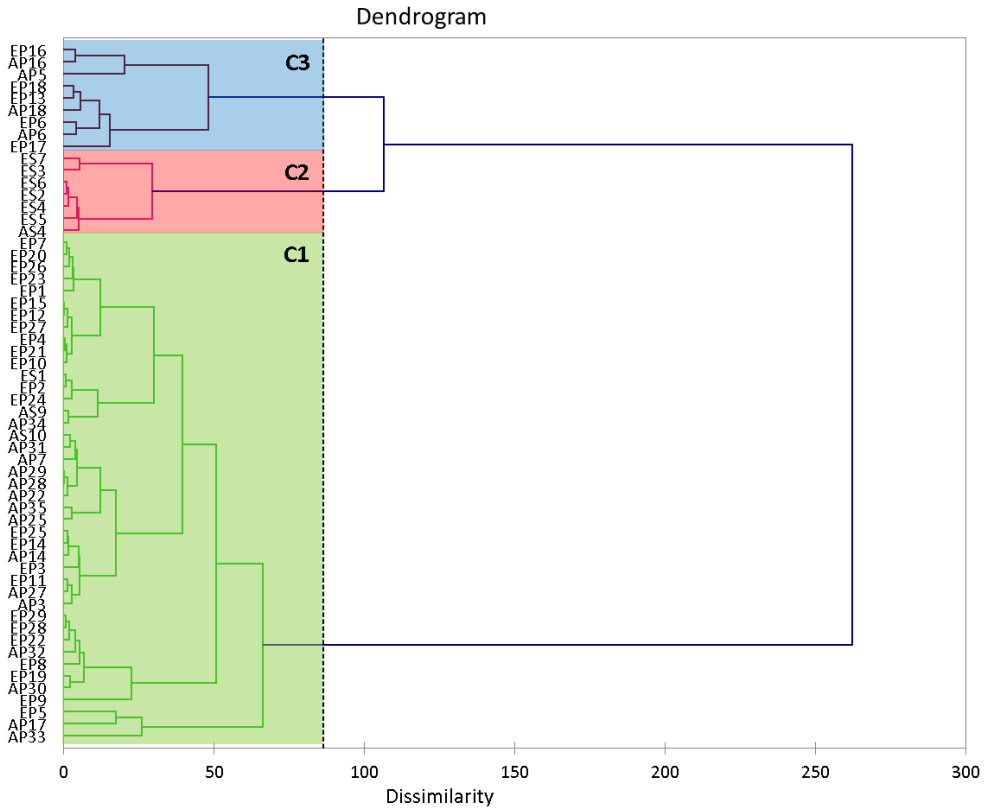

Figure 5. Dendrogram obtained by hierarchical clustering analysis HCA .

The C3 includes 10 samples located in the south-western border of the area, near the active volcanic complexes. Their similarity could support the hypothesis of a common evolutional trend related to the recent volcanic history of this area. Two samples (AP5 and AP16) correspond to those points that belong to the Cl-SO_4-Ca-Mg type showed in Piper diagram (Figure 3). Three couples (EP18-AP18, AP6-EP6, AP16-EP16) represent the same sampling points in two different years. The good agreement of chemical features among the two sampling campaigns reflects unchanged chemical characteristics of the groundwater collected in those points. Conversely, AP17 and EP5, that are the same sampling points of respectively EP17 and AP5 found in C3, are located in cluster C1. This

485 indicates an inter-annual variability for these points that can be explained with a decreasing ion
486 concentration and EC from 2011 to 2012, likely due to the fact that the samples of 2012 were
487 collected in May, at the beginning of the rainy season, while the 2011 samples in February during
488 the dry season (see Table 1) and thus the azimuthal groundwater recharge regime was different.
489 The HCA revealed the possibility of recognizing a geographical criterion among sampled
490 groundwater. Nevertheless, a more detailed focus is needed on the parameters influencing the
491 sampled waters and thus a PCA was performed. Figure 6 shows the combined plot of scores and
492 loadings obtained by PCA considering the waters collected in both sampling campaigns. Taking
493 into account the scree plot, we reported only the first two principal components that contain a total
494 variance of about 62 %; the remaining PCs contain a low, and therefore not significant, percentage
495 of information.
496 Regarding the variables, a correlation among the main dissolved species (major ions, EC, TDS) and
497 the PC1 is evident. Furthermore, all the samples collected in the area near the active volcanic
498 complexes (cluster C3) are distributed along the positive PC1 axis. O_2 and O_2% variables are
499 represented by vectors having opposite direction relative to pH and T variables on PC2. This
500 indicates that high concentrations of dissolved oxygen appear with low pH and temperature. K^+, Pb
501 and Mn variables are characterized by vectors having different directions with respect to those of
502 the other variables, indicating a their uncommon behavior in the different aquatic systems
503 considered.
504 Clusters derived from HCA were overlapped as coloured areas in order to compare the two
505 chemometric approaches and to associate the physico-chemical parameters to the clusters detected
506 by HCA. The cluster C1, representing waters collected in the central sector of Xela caldera, are
507 weakly influenced by the main chemistry of groundwater, since they are located to the opposite side
508 of TDS, EC and main ions vectors. This is probably linked to the fact that they are more diluted
509 than the groundwater close to volcanic area, where sampled waters (cluster C3) have higher
510 contents of solutes. Hence, their origin might be related to different flow paths that are composed by

511 more diluted groundwater infiltrated in recharge areas. Conversely, some points belonging to C1 of
512 HCA (EP5, EP9, EP19, AP17, AP25, AP30) lay on the right side of PC2 axis, indicating that they
513 might be influenced by the main dissolved species. Among these, AP33 and AP17 occupy a
514 separated position in the lowermost part of the plot because of low O_2 concentrations. This explains
515 particularly the different position for AP17 and EP17 samples: even though collected in the same
516 well, they show a relevant decrease in O_2 concentration in one year (from 5.16 to 1.98 mg/L). As in
517 the case of sample AP33, that remains isolated because of its high temperature and low O_2
518 concentration, low oxygen values may be explained by the presence of organic pollutants in
519 aquifers, linked to local inputs from wastewater discharges.
520 The group C2, formed by spring waters, is well identified also in PCA, as it is greatly influenced by
521 the variables identified by the vectors of the dissolved oxygen. This is confirmed by the high values
522 of O_2 found in those waters (6.47÷6.89 mg/L).
523 The samples in cluster C3 are relatively scattered but the behaviour is quite homogeneous since
524 they occupy the leftmost part of the plot. They are strongly dependent on the main dissolved ionic
525 species because they are aligned with the direction of the vectors representing the major ions, CE
526 and TDS. As in HCA, differences among the two years of sampling can be found, but this does not
527 significantly affect their position. An exception is represented by AP17 and EP5: in HCA they were
528 listed in C1 but they see to be much close to their correspondents EP17 and AP5 the EP5 sample
529 can be here considered belonging to the C3 cluster. The analyses results (Table 2) confirm the
530 similarity between EP5 and samples belonging to C3 cluster.
531 Table 4 presents the factor loadings obtained for the groundwater samples collected in the
532 investigated area. Four factors were obtained summing more than 70% of the total variance in the
533 entire data set. The first factor, accounting for 42% of the total variance, presents highest loading
534 for EC, Ca^{2+}, Mg^{2+}, Na^{+}, HCO_3^{-}, SO_4^{2-}, Cl^{-}, NO_3^{-}, TDS. Hence, this factor represents the main
535 components of groundwater. The second factor is characterized by high loadings of dissolved
536 oxygen and Pb^{2+}. For this reason we hypothesized that this factor describes the behavior of the

oxygenated groundwater usually more rich in heavy metals such as lead. Indeed lead is often found in sediments like sulfide in reducing conditions but it can be released into the waters under oxidizing conditions due the fact that the sulfidic component is oxidized to sulfate. In factor 3 pH, temperature and HCO_3^- have a positive factor loading: this indicates a strong interconnection among these variables. This finding confirms the strict dependence of bicarbonate equilibrium on pH and temperature: neutral or slightly acid or basic conditions foster HCO_3^- dissolution, while at constant pH HCO_3^- is more soluble at low temperatures. Finally the last factor presents high and moderate loading for K^+ and Mn respectively. It can be then associated with the behavior of some groundwater characterized by relatively high concentration of potassium and, to a lesser extent, manganese but not of other principal ions. Such finding is partially confirmed by the presence in analyses results of samples with K^+ concentrations >3 mg/l and moderate concentrations of other ionic species. This suggests the presence of an independent source of K^+ in the considered groundwater system. Considering that these are few cases and that the main rock formations are sources of Na^+, the source may be anthropogenic and with local significance, for instance nutrient-related inputs.

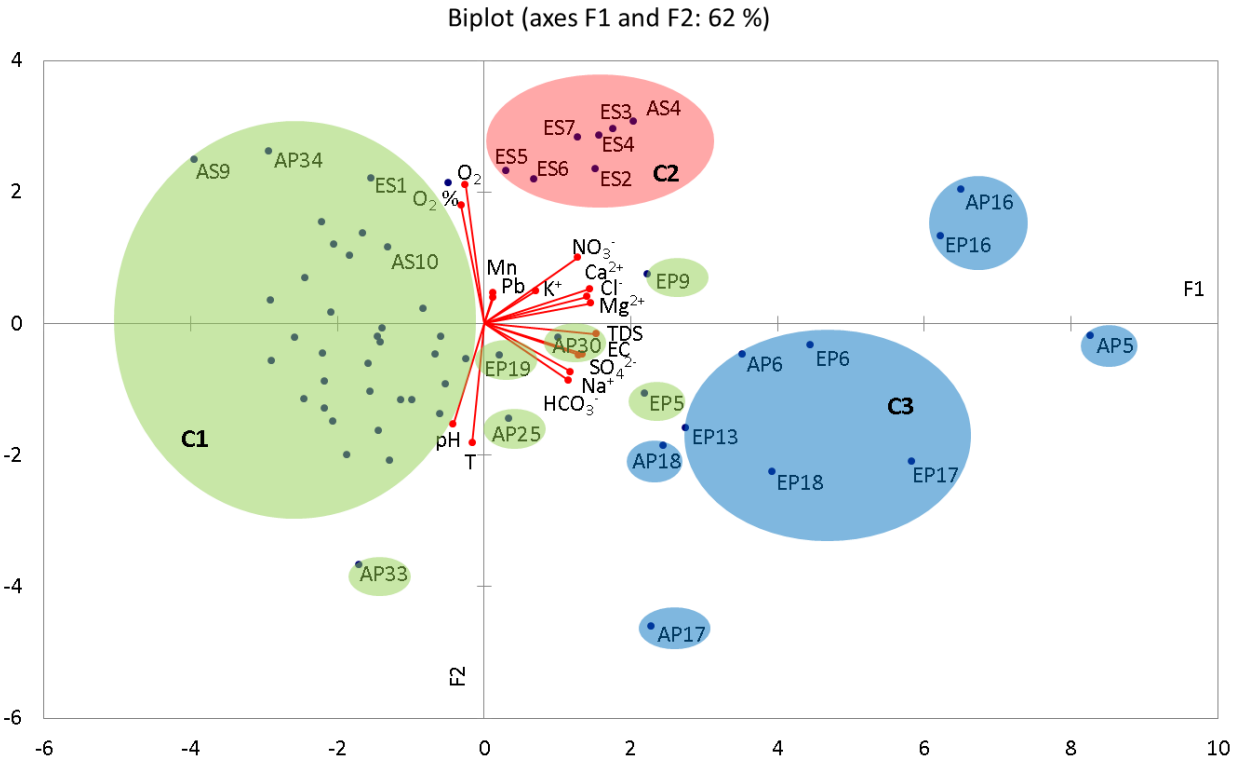

552

553 Figure 6. Biplot obtained by principal component analysis PCA. Coloured areas correspond to the

554 clusters detected in hierarchical clustering analysis HCA.

555

556 **Table 4.** Variable loadings in the factors obtained by FA for groundwater samples. The bold values

557 correspond for each variable to the factor having the largest cosine square

558

Variables	F1	F2	F3	F4
T	-0.142	-0.408	**0.515**	-0.131
E.C.	**0.871**	-0.241	0.022	-0.200
pH	-0.263	-0.219	**0.592**	-0.282
O2 %	-0.103	**0.895**	0.010	-0.025
O2	-0.064	**0.984**	-0.165	0.034
Ca^{2+}	**0.918**	0.104	-0.037	0.230
Mg^{2+}	**0.929**	0.071	0.047	0.106
Na^{+}	**0.706**	-0.224	0.257	-0.033
K^{+}	0.338	0.004	-0.037	**0.728**
HCO_3^{-}	**0.681**	-0.160	**0.644**	0.195
SO_4^{2-}	**0.786**	-0.236	0.088	-0.006
Cl^{-}	**0.895**	-0.054	-0.265	0.097
NO_3^{-}	**0.831**	0.163	-0.367	0.143
TDS	**0.967**	-0.079	0.204	0.131
Pb	0.123	**0.337**	0.279	-0.159
Mn	0.050	0.076	-0.044	**0.199**

559

560 ## 5. CONCLUSIONS

561 The present study aimed to improve the knowledge of the hydrochemical setting of a large area in
562 central America, where groundwater features were almost unknown.The hydrochemical results
563 show the prevalence of the meteoric influence, according to the Ca-Mg-HCO3 facies. Further
564 processes such as mixing with hydrothermal fluids in the volcanic areas and ion exchange with clay
565 minerals in the aquifer solid matrix, are likely responsible for the Na enrichment of some waters.
566 Along with that, a Mg enrichment was also detected in the southern sector, due to the circulation in
567 the andesitic rocky complexes of Santa Maria and Cerro Quemado volcanic complexes.
568 Furthermore, anthropogenic inputs were detected: nitrates in rural areas and lead in urban areas that
569 in some cases are above the quality standards.
570 The research highlighted the importance of coupling Piper and Schoeller diagrams and univariate
571 plots with chemometric tools (PCA and HCA). From one side the hydrochemical facies of
572 groundwater were defined and the reason for different water composition were hypothesized, while
573 on the other side the multivariate analysis allowed to better distinguish more features of
574 groundwater thanks to the comparison between physical and chemical parameters. HCA revealed
575 that the majority of samples can be ordered following a geographical criterion and PCA allowed a
576 more detailed focus on the parameters influencing the analysed waters. Principal ions, as well as
577 oxygen content, were envisaged as the most discriminating parameters influencing the water
578 composition. The latter is possibly influenced by the presence of organic contamination and by the
579 temperature value. Furthermore, data evidenced the almost complete absence of contamination
580 sources for toxic heavy elements, with only two exceptions (nitrate and lead), likely connected to
581 agriculture and urban wastewater.
582 This first chemical characterisation of the area may be used by both researchers for further studies
583 and by the stakeholders for the management of groundwater, for instance posing the basis for the
584 development of a groundwater monitoring network.
585

586 **6. Acknowledgements**

This study has been carried out thanks to ATO3 and UNICOO projects supported by Municipality and University of Turin. Authors are grateful to H.O. Hernandez Sac (CUNOC-*Centro Universitario de Occidente*) and to EMAX staff (*Empresa Municipal de Aguas de Xelajù*) for field support.

7. References

Adams, A., Goff, F., Trujillo, P.E. Jr, Counce, D., Archuleta, J., Dennis, B., Medina, V., 1990. Hydrogeochemical investigations in support of well logging operations at the Zunil geothermal field, Guatemala. Geothermal Resources Council Transactions, 14 (II):829-835.

Agrawal, G.D., Lunkad, S.K., Malkhed, T.M, 1999. Diffuse agricultural nitrate pollution of groundwaters in India. Water Sci Technol 39(3):67-75.

Appelo, C.A.J., Postma D., 1996. Geochemistry, groundwater and pollution. Balkema, Rotterdam, p 536.

Asturias, F., 2003. Reservoir assessment of Zunil I and II geothermal fields, Guatemala. The United Nations University Geothermal Training Program, Report 3. http://www.os.is/gogn/unu-gtp-report/UNU-GTP-2003-03.pdf

Bennati, L., Finizola, A., Walker, J.A, Lopez, D.L., Higuera-Diaz, I.C., Schutze, C., Barahona, F., Cartagena, R., Conde, V., Rios, C., 2011. Fluid circulation in a complex volcano-tectonic setting, inferred from self-potential and soil CO_2 flux surveys: The Santa María–Cerro Quemado–Zunil volcanoes and Xela caldera (Northwestern Guatemala). J. Volcanol. Geoth. Res. 199 (3-4):216-229.

Bucci, A., Franchino, E., Bianco Prevot, A., Lasagna, M., De Luca, D.A., Hernandez Sac, H.O., Macario, I., Sac Escobar, E.O., 2015. Hydrogeological and hydrochemical study of Samalá River Basin, Quetzaltenango area, south western Guatemala. G. Lollino et al. (eds.), Engineering Geology for Society and Territory – Volume 3, River Basins, Reservoir Sedimentation and Water Resources, 245-248. Springer International Publishing Switzerland 2015. doi: 10.1007/978-3-319-09054-2_50

612 Cáceres, D., Monterroso, D., Tavakoli, B., 2005. Crustal deformation in northern Central America.
613 Tectonophysics 404:119–131.
614 Cepal, 2002. Desafíos y propuestas para la implementación más efectiva de instrumentos
615 económicos en la gestión ambiental de América Latina y el Caribe. United Nations Publications,
616 Santiago de Chile.
617 http://repositorio.cepal.org/bitstream/handle/11362/5572/S0210017_es.pdf?sequence=1
618 CIA (Central Intelligence Agency), 2014. The world factbook. Guatemala. Visited on 9th of April
619 2014. https://www.cia.gov/library/publications/the-world-factbook/geos/gt.html
620 COGUANOR NGO 29 001, 1999. AGUA POTABLE, Especificaciones. Diario Oficial de Centro
621 América, 2000-02-04.
622 Conway, F.M., Vallance, J.W., Rose, W.I., Johns, G.W., Paniagua, S., 1992. Cerro Quemado,
623 Guatemala: the volcanic history and hazards of an exogenous volcanic dome complex. J. Volcanol.
624 Geoth. Res. 52 (4):303–323.
625 Conway, F.M., Diehl, J.F., Rose, W.I., Matías, O., 1994. Age and magma flux of Santa Maria
626 Volcano, Guatemala: correlation of paleomagnetic waveforms with the 28,000 to 25,000 yr B.P.
627 Mono Lake Excursion. J. Geol. 102:11-24.
628 Davis, S.N., DeWiest, R.J.M., 1966. Hydrogeology. John Wiley & Sons, New York, U.S.A.
629 Duffield, W., Heiken, G., Foley, D., McEwen, A., 1993. Oblique synoptic images, produced from
630 digital data, display strong evidence of a “new” caldera in south-western Guatemala. J. Volcanol.
631 Geoth. Res. 55(3–4):217–224.
632 Einax, J.W., Zwanziger, H.W., Geiβ S., 2004. Chemometrics in Environmental Analysis. Wiley-
633 VCH, Weinheim.
634 Fetter. C.W., 2001. Applied hydrogeology. Pearson/Prentice Hall, Edinburgh Gate, England.
635 Foley, D., Moore, J.N., Lutz, S.J., Palma, J.C., Ross, H.P., Tobias, E., Tripp, A.C., 1990. Geology
636 and geophysics of the Zunil geothermal system, Guatemala. Geothermal Resource Council -
637 Transactions, 14, 1405–1412.

638 Fournier R.O., 1981. Applications of water geochemistry to geothermal exploration and reservoir
639 engineering. In Rybach L. and Muffler L.J.P., eds, Geothermal Systems: Principles and Case
640 Histories: New York, John Wiley, 109-143.
641 Franchino, E., De Luca, D.A., Bianco Prevot, A., Lasagna, M., Hernandez Sac, H.O., 2013.
642 Hydrogeological study of Quetzaltenango area (southwestern Guatemala), Rend. Online Soc.
643 Geol. It. 24:137-139.
644 Goff, E., Janik, C.J., 2000. Geothermal systems, in Encyclopedia of Volcanoes, edited by:
645 Sigurdsson H., Houghton B., McNutt S., Rymer H., and Stix J., Encyclopedia of Volcanoes: San
646 Diego, Academic Press, 817-834.
647 INSIVUMEH (Instituto Nacional de Sismología, Vulcanología, Meteorología e Hidrología), 1988.
648 Informe final estudio de aguas subterráneas en el valle de Quetzaltenango (Mapas). Proyecto:
649 estudio de aguas subterráneas en Guatemala.
650 Kim, J.H., Kim, R.H., Lee, J., Jehong, T.J., Yum, B.W., Chang, H.W., 2005. Multivariate statistical
651 analysis to identify the major factors governing groundwater quality in the coastal area of Kimje,
652 South Korea. Hydrol. Process. 19:1261–1276.
653 Kim, T.H., Chung, S.Y., Park, N., Hamm, S.Y., Lee, S.Y., Kim, B.Y., 2012. Combined analyses of
654 chemometrics and kriging for identifying groundwater contamination sources and origins at the
655 Masan coastal area in Korea. Env. Earth Sci. 67(5):1373-1388.
656 Lima Lobato, E.M., Palma J., 2000. The Zunil-II geothermal field, Guatemala, Central America.
657 Proceedings of the World Geothermal Congress, Tohoku, Japan, 2133–2138.
658 MARN-URL/IARNA-PNUMA (Ministerio de Ambiente y Recursos Naturales), 2009. Informe
659 Ambiental del Estado - GEO Guatemala 2009. http://www.sia.marn.gob.gt/Documentos/geo09.pdf.
660 Montcoudiol, N., Molson, J., Lemieux J.-M., 2015. Groundwater geochemistry of the Outaouais
661 Region (Québec, Canada): a regional-scale study. Hydrogeol. J. 23:377-396.
662 Möller, D., 1990. The Na/Cl ratio in rainwater and the seasalt chloride cycle. Tellus 42B, 254-262.

663 Nagaraju, A., Sunil Kumar, K., Thejaswi, A., 2014. Assessment of groundwater quality for
664 irrigation: a case study from Bandalamottu lead mining area, Guntur District, Andhra Pradesh,
665 South India. Appl. Water Sci. 4:385–396.
666 Neal, C., Kirchner, J.W., 2000. Sodium and chloride levels in rainfall, mist, streamwater and
667 groundwater at the Plynlimon catchments, mid-Wales: inferences on hydrological and chemical
668 controls. Hydrol. Earth Syst. Sci. 4(2):295-310.
669 Ortega-Obregón, C., Solari, L., Keppie, J.D., Ortega-Gutiérrez, F., Solé J., Morán-Ical S., 2008.
670 Middle-Late Ordovician magmatism and Late Cretaceous collision in the southern Maya block,
671 Rabinal–Salamá area, central Guatemala: implications for North America–Caribbean plate
672 tectonics. Geol. Soc. Am. Bull. 120(5-6):556–570.
673 Otto, M., 2007. Chemometrics, 2nd Edition, Wiley-VCH, Weinheim.
674 Piper, A.M. (1944). A graphical interpretation of water—analysis. Trans. Am. Geophys. Union.
675 25:914–928.
676 Phipps Morgan, J., Ranero, C.R., Vannucchi, P., 2008. Intra-arc extension in Central America:
677 Links between plate motions, tectonics, volcanism, and geochemistry. Earth Planet. Sc. Lett.
678 272:65–371.
679 Spitz, K., Moreno, J., 1996. A practical guide to groundwater and solute transport modeling. Ed.
680 John Wiley & Sons, New York. 461 pp.
681 Rose, W.I. JR, Grant, N.K., Hahn, G.A., Lange, I. M., Powell, J.L., Easter J, Degraff, J.M. (1977)
682 The evolution of Santa Maria volcano, Guatemala. Journal of Geology 85:63-87.
683 Rose, W.I, 1987. Volcanic activity at Santiaguito Volcano, 1976–1984. Geol. Soc. Am. Special
684 Paper 212:17–27.
685 Schoeller, H., 1967. Qualitative evaluation of groundwater resources. In: Methods and techniques
686 of groundwater investigation and development. Water Res. UNESCO 33:44–52.
687 Schoeller, H., 1977. Geochemistry of groundwater. In: Groundwater studies—an international guide
688 for research and practice. UNESCO, Paris, 15:1–18

689 SEGEPLAN (Secretería de Planificación y Programación de la Presidencia de la República de
690 Guatemala) – BID (Banco Interamericano de Desarrollo), 2006. Estrategia para la gestión integrada
691 de los recursos hídricos de Guatemala. http://www.marn.gob.gt/sub/portal_samya/docs/sdag.pdf
692 Smeti, E.M., Thanasoulias, N.C., Lytras, E.S., Tzoumerkas, P.C., Golfinopoulos, S.K., 2009.
693 Treated water quality assurance and description of distribution networks by multivariate
694 Chemometrics. Water Res 43:4676–4684.
695 Walker, J.A., Templeton, S., Cameron, B.I., 2006. The chemistry of spring waters and fumarolic
696 gases encircling Santa María volcano, Guatemala: insights into regional hydrothermal activity and
697 implications for volcano monitoring. Geol. Soc. Am. Special Paper 412:59-83.
698 White, D.E., 1957. Thermal waters of volcanic origin. Geol. Soc. Am. Bull. 68:1637-1682.
699 Williams, H., 1960. Volcanic history of the Guatemalan Highlands. U. Calif. Geol. Sci. 38:86-90.